Realization of a double pump parametric amplifier

A Semesterthesis by
CHRISTA FLÜHMANN

supervised by
Prof. Andreas Wallraff
Christopher Eichler

October 18, 2011
Quantum Device Lab,
ETH Zürich

Abstract

The double pump Josephson parametric amplifier is discussed and realized. A model based on the differential equation for the node flux of a circuit system is presented. In addition the experimental setup used and the measurement method is summarized. In the experiment similar amplification characteristics as in the single pump case are obtained. As well as a test of phasesensitive amplification with two pump drives is performed. The double pump amplification is further analyzed on its dependence on the frequency spacing of the two pump drives.

Contents

Chapter 1

Introduction

The Interaction of matter and light is a fundamental physical problem. The most elementary question is how one single photon interacts with only one atom. This problem can be studied in different ways. One possibility is the so called Circuit Quantum Electrodynamics (Circuit QED). In doing so neither a real atom nor electromagnetic waves in the visible spectrum are used. Rather an artificial alternative system is studied. A quantum mechanical system with two energy level for example realized as a Cooper-Pair-Box is used as artificial atom. This is explored in a quasi one dimensional microwaves resonator. With such a system strong interaction of light and matter can be studied. 2004 A. Wallraff et al. first demonstrated this strong interaction in Yale [1].
A microwave photon has much less energy (factor $\approx 10^6$) than a photon from the visible spectrum. Thus it is much harder to detect a microwave photon. To detect microwave signals gallium arsenide hetero-structures as MESFETS and mostly HEMTs (High electron mobility transistors) are used as amplifiers. To further improve the amplification an ultra low noise amplifier to put in front of an HEMT is searched. A promising candidate for such an low noise amplifier is the Josephson parametric amplifier.
In a typical parametric amplifier process an input signal is increased by energy transfer from a pump drive. This energy transfer can also be realized by two pump drives with two different frequencies. The goal of this semesterthesis is to realize amplification with two frequencies and to analyze the advantages of the double pump amplifier.

Chapter 2

Parametric amplifier

The damped driven harmonic oscillator is a well known physical problem. The damping constant and the resonance frequency are characteristic parameters of it. If these parameters become variable, for example a time depending damping constant, then a parametric oscillator is obtained. This system also shows resonance phenomena and because of its non-linearity frequency mixing may occur. Such a system can be used to amplify signals. In a typical parametric amplifier process which is shown in figure 2.1 the incoming signal with amplitude A_s^{in} interacts with a pump drive of amplitude A_p^{in} [2]. The signals amplitude is increased due to an energy transfer from the pump drive and reflected back as output with increased amplitude A_s^{out}. Due to the energy transfer to the signal the pump drive depletes. In this process a second wave at a different frequency is produced and leaves the amplifier the so called idler.
The goal of this project is to realize this amplification process with two pump drives instead of one.

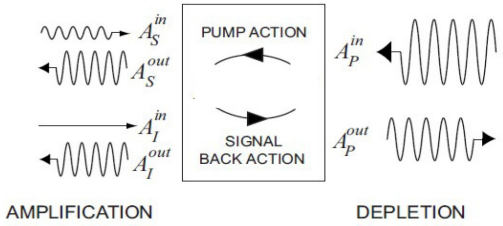

Figure 2.1: ***Typical parametric amplifier process****: Increase of signal amplitude due to energy transfer from a pump drive and creation of the idler frequency. [2]*

2.1 Advantage of amplification with two pump drives

Parametric amplifiers are interesting to explore because they provide a possibility of ultra low noise amplification. As already mentioned one way to realize a parametric amplifier is with the help of two different pump frequencies.
Figures 2.2 and 2.3 show the schematics of typical noise power spectral densities for single and double pumped amplifiers. The coordinate Δ displays the difference of the frequency to the resonance frequency. There is an overall offset colored transparently on both pictures. This is the system noise, which is always present. Then there are sharp and high peaks which correspond to the pump drives. Also the Lorenz shaped amplified signal shown. With a filter, drawn in red, the data which is analyzed is chosen.
In figures 2.2 and 2.3 the example of phase sensitive amplification is shown. In a phase sensitive measurement the pump and signal frequency lie exactly at the resonance frequency. Also a symmetric filter is used such that the same amount of signal and idler quadratures are measured. This gives the possibility of amplify the signal quadrature noiselessly with the cost of attenuate the idler quadrature.
In the single pump case (figure 2.2) the pump drive lies in the region of the filter and thus appears in the measured data. This is unwanted and can be avoided with two pump drives. The detuning (frequency spacing) of the two pump frequencies is chosen such that they lie at null-points of the filter (see figure 2.3). The pump drives are simply filtered away and thus do not appear in the data. This is the main advantage of using two pump drives.

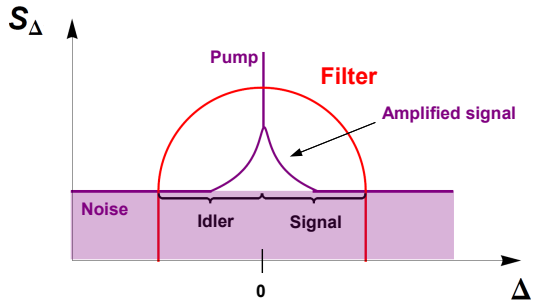

Figure 2.2: ***Noise spectral density with a single pump drive****: Shown are the Pump,the amplified signal,the system noise and the filter; The pump drive lies in the region of the filter and thus appears in the measurement data; Δ displays the difference to the resonance frequency*

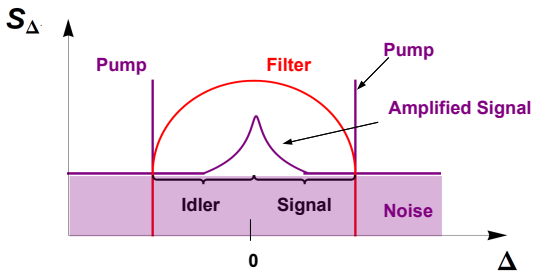

Figure 2.3: ***Noise spectral density with two pump drives****: Shown are the Pump drives, the amplified signal, the system noise and the filter; The frequencies of the two pump lie at a null-point of the filter and do not appear in the measurement data; Δ displays the difference to the resonance frequency*

2.2 Realization of a parametric amplifier

One version of a parametric oscillator is based on a current depending inductance L. In the experiment a quasi one dimensional microwave resonator is used. The sample is shown schematically in figure 2.4. Superconducting areas are shown in light blue, while the white spaces indicate isolating parts. The isolating parts act as capacitance. In the end of the sample is an array of superconducting interference devices (SQUIDs). They provide the non linear inductance of the system.

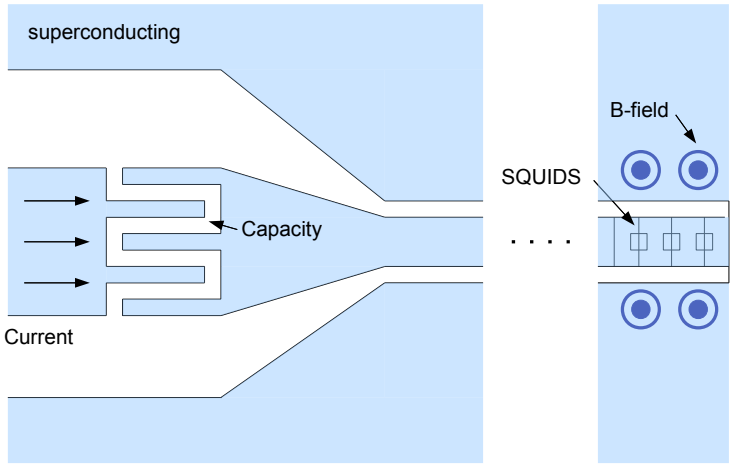

Figure 2.4: ***Microwave resonator:*** *blue parts are superconductive; white parts indicate nonconducting areas, which act as capacitance; There is a SQUID array in the end. The magnetic flux through the SQUIDs can be varied with a coil below the sample*

A SQUID is a superconducting ring with two small non-conducting barriers called Josephson junctions. As consequence of the flux quantization through such a ring, the current voltage characteristics is nonlinear. The relation is approximately sinusoidal and can be expanded in a Taylor series:

$$I(t) = I_0 \sin(\frac{2e}{\hbar}V) \qquad \approx \frac{2e}{\hbar}I_0 V + \frac{1}{6}(\frac{2e}{\hbar})^3 I_0 V^3 \tag{2.1}$$

Considering only the first two terms a SQUID can be approximately described as:

$$\begin{aligned} I &= \frac{1}{L}V && \text{for any inductance} \\ L &= L_j + \delta L && \text{for the SQUID with:} \\ L_j &= \frac{2e}{\hbar}I_0;\ \delta L = \frac{1}{6}L_j\frac{I^2}{I_0^2} \end{aligned} \tag{2.2}$$

Below these SQUIDS a coil is attached, which gives the possibility of changing the inductance by a magnetic field. Changing the inductance implies a change of the resonance frequency and thus a tunable amplifier.
In the superconducting regions a current is conducted to the sample. The current induces electromagnetic fields in the non-conducting parts which again induce currents in the resonator. Therefor the current manages to overcome the non-conducting cap. The current is reflected back and forth in the resonator and in each turn a certain amount leaves the system at the capacity.
One important characteristics of such a parametric amplifier is the quality factor. The quality factor is a measure of the damping, meaning the energy losses of the system. The quality factor is defined as the resonance frequency times the ration between energy stored in the system to the dissipated energy in one cycle:

$$Q_L := \omega_{res}\frac{\text{Stored Energy}}{\text{Dissipated Energy}} = \omega_{res}\frac{\overline{n}\hbar\omega_{res}}{P_{out} + P_{loss}} \tag{2.3}$$

It is convenient to split up the quality factor in an internal- and an external part. The internal quality factor revering to losses in the system while the external describes the losses due to out coupling.

$$\begin{aligned} Q_{int} &= \omega_{res}\frac{\overline{n}\hbar\omega_{res}}{P_{loss}} \\ Q_{ext} &= \omega_{res}\frac{\overline{n}\hbar\omega_{res}}{P_{out}} \\ \frac{1}{Q_L} &= \frac{1}{Q_{int}} + \frac{1}{Q_{res}} \end{aligned} \tag{2.4}$$

2.3 Basic model of the parametric amplifier

The whole microwave resonator system can be described by a parallel LRC-circuit with a non-linear inductance which is shown in figure 2.5 [2]. Indicated on the figure are the different currents in the system: The two pump drives, the signal current and the noise.

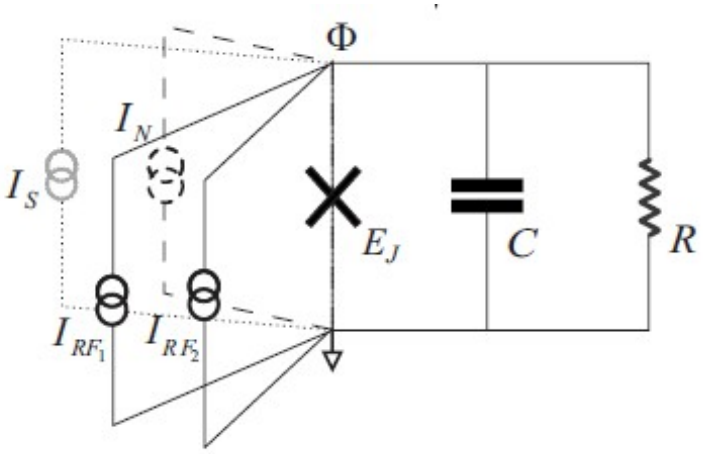

Figure 2.5: ***Description of the microwave resonator by a parallel LRC-circuit****: with non-linear inductance E_j, the two pump currents I_{RF1} and I_{RF2}, the signal current I_s and the noise current I_N; shown as well are the capacitance C and the resistance R [2]*

Such a circuit can be described by a differential equation with only one degree of freedom, the node flux. This variable is defined as the sum of branch fluxes connecting the node with the defined ground node. One such branch flux is the integral over the time since $-\infty$ of the instantaneous flux through the branch. For more details to the exact definitions and the derivation of such an differential equation see the text [3]. The differential equation for the circuit in figure 2.5 is given by:

$$\ddot{\Phi} + 2\Gamma\dot{\Phi} + \omega_0^2(1 + \lambda(\frac{2\pi\Phi}{\Phi_0})^2) = \frac{1}{C}(I_{RF1}\cos(\omega_1 t) + I_{RF2}\cos(\omega_2 t) + I_N)[2] \tag{2.5}$$

The second term describes the decay in the resonator with the damping constant Γ as characteristic parameter. The non-linearity is put into the formula via the non-linearity coefficient λ. For a SQUID this constant is $\lambda = \frac{1}{6}$. With the help of this constant the

formula can be extended to different non-linearity as for example an array of SQUIDs as in our case. There are also two terms describing the pump drives with strengths I_{RF1}, I_{RF2} and frequencies ω_1 and ω_2. The last term considers the input signal.
To solve the differential equation an appropriate ansatz which contains the possible input frequencies is inserted. Afterward harmonic balance for signal, idler an the two pump frequencies is performed. In doing so several approximations are considered. A system of equations is obtained. They are further simplified to linear equations under the stiff pump approximation where back action is neglected and the total pump strength is assumed to be constant. The output fields are calculated from the fields in the resonator with the help of input output theory. More details to this calculation are found in the appendix. The derivation are based on the work from A. Kamal, A Marblestone and M. Devoret in the Physics Review B 79 [2].

2.4 Measurement setup and method

In principle the properties of the sample are investigated as follows: Microwave signals are generated and conducted to the sample in the cryostat. They couple into the resonator and are reflected back and forth. A part of the field in the resonator is coupled out and analyzed.
The experimental setup is given in figure 2.7. Three generators are connected via microwave coaxial cables to the sample. Three generators are needed one to generate the signal and the other two to drive the system when the double pump is tested. Their signal are added together. Afterwards it is split up in two equal parts one as reference channel and the other going to the sample in the vericold dilution refrigerator.
The temperature at the level of the sample can be cooled down to 20 mK. This low temperature is needed to reach the quantum regime. If the thermal energy is smaller than the energy quantum associated with the resonance frequencies of the resonator $k_bT \leq \hbar\omega_{res}$ then measurements in the quantum regime are possible.
The low temperature in the cryostat is cooled down in several temperature steps in each step the wires connected to the sample should not transport more thermal energy than the cryostat can cool down. For this reason special coaxial-cables out of stainless steel are used in the cryostat. They are bad thermal conductors but also add more attenuation. This attenuation would be too much for the weak output signal that's why for the output a special cable is used. In each step the components have to be thermalized this is done with cooper wires attached to the different devices.
Before the signal reaches the cryostat different attenuators are built into the setup to diminish the power enough such that the sample can not be damaged. To hold losses as small as possible the measurement is done in reflection. This means that at the same capacity where the signal couples into the resonator the reflected signal is measured. To distinguish the incoming and the outgoing signal a circulator is used. The circulator has three ports the incoming signal is always going to the next port in anticlockwise rotation.

To analyze the outgoing signal a IQ-mixer is used to down convert to smaller frequencies. A IQ - mixer consist out of two mixers. A mixer combines two frequencies. The input signal and a so called local oscillator signal. The output signal of a mixer contains other frequencies like the sum and the difference of the input signals. With filters one can choose the frequencyband which is useful for the further application. This is visualized in figure 2.6 on the left. In the case of a IQ mixer (figure 2.6 on the right) the local oscillator signal is first split up in two parts. To one part a phase of 90° is added. The local oscillator signals are then mixed with the split up radio frequency. Which yields two different signals f_i , f_q leaving the IQ mixer. In this case the high RF frequency is converted to smaller frequencies which are easier to analyze.

This so called I an Q quadratures are then amplified, digital to analogue converted and

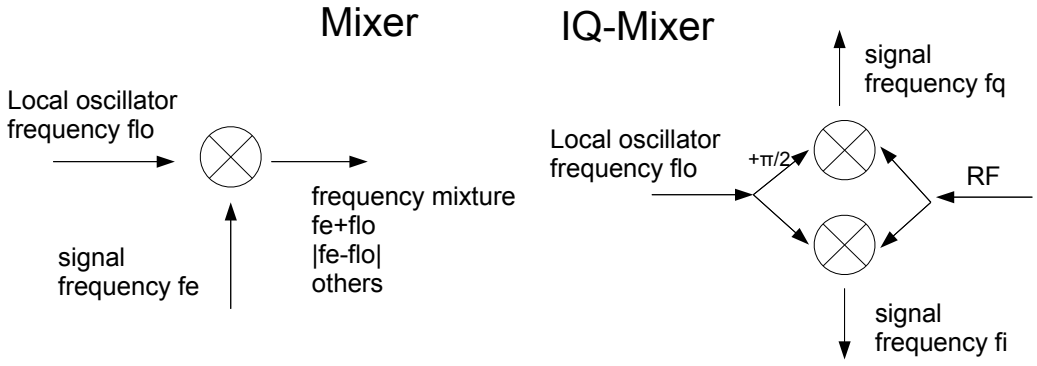

Figure 2.6: ***Principle of a mixer and IQ-Mixer****: A mixer combines two signals and produces the sum and the difference of the two frequencies. A mixer can be used to down convert frequencies to smaller ones, a IQ mixer consists of two mixers and can also be used to down convert*

analyzed with the help of a field-programmable gate array (FPGA). From the measured quadratures one can conclude back to the properties of the resonator.

Data is measured for 25μs. This is done many times and the results are averaged. With this technique one can get rid of the noise. Because of the length of the measurement interval all frequencies which are no multiples of 40 kHz are averaged out. Thus the signal frequency is chosen as multiples of 40 kHz. In contrast the pump drives and the idler are chosen such that they are averaged out.

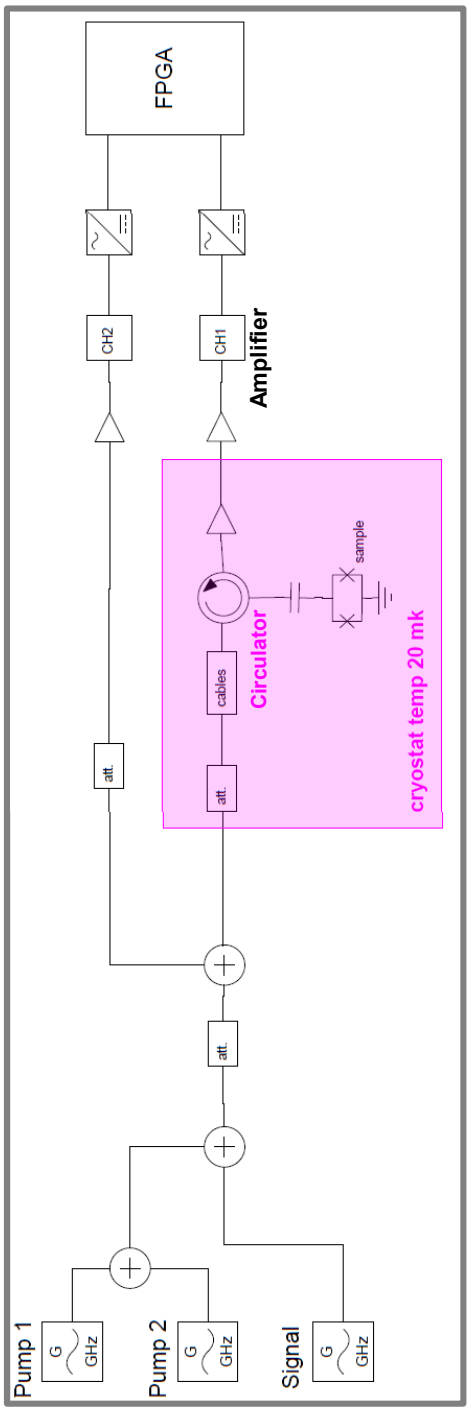

Figure 2.7: ***Experimental Setup:*** *Shown are the three generators connected via coaxial cables to the sample in the cryostat, to distinguish incoming and outgoing signals a circulator is used, the data is amplified and analyzed in the field programmable gate array FPGA*

Chapter 3

Measurement results and analysis

3.1 The sample: Tunability and quality factor

First the sample is characterized especially important is its tunability, the dependence of the resonance frequency on the voltage of the coil. The range of possible resonance frequencies shows how good the amplifier can be tuned. Only signals with a frequency near the resonance frequency are amplified hence it is favorable to have a high tuneability. To measure this effect a coherent signal is conducted to the resonator where the coil generated a magnetic filed. The increase of the signals amplitude is measured. This is done for different combinations of coil voltages and frequencies.
The results are given in figure 3.1. In blue the measurements results are displayed, plotted in red is a model calculation. The model is in good agreement with the measurement especially between -0.2 V to 0.15 V. resonance frequencies between 3 GHz to 6.8 GHz are observed. From this data the quality factor is calculated via formula 2.4. The results are given in figure 3.2. At zero voltage on the coil a quality factor of about 247 is found. At this point the sample was designed to have a quality factor of 300.

3.2 Equivalence of single and double pump amplification

The next task is to achieve typical amplification characteristics with one as well as with two pump drive. It is also important to check whether it is possible to observe the same results in both cases.
To do so the region around the resonance frequency is examined. The gain is measured for different combinations of pump-powers and frequencies. In the case of one pump drive this is done as showed in figure 3.3. The pictograph in figure 3.3 with the arrows illustrates

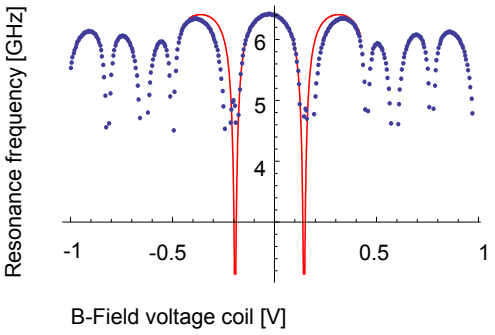

Figure 3.1: ***Resonance frequency dependence on the flux through the SQUIDS*** *Blue: Measurement, Red: Model fit*

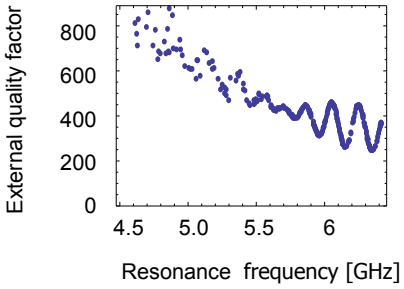

Figure 3.2: ***External Quality factor for different resonance frequencies***

the measurement technique. An arrow stands for a certain signal its height corresponds qualitatively to its power and its horizontal location to the frequency. Black variables stay constant during the measurement while purple ones are swept. The values of the constant variables are given on the right. This means in figure 3.3 two signals are generated a much stronger pump drive and a weak signal their frequency spacing stays constant at 10 kHz during the measurement. The power of the pump and the frequency of both signals are varied. Measured is the gain of the signals amplitude in the output.
The results are presented as density plot. Combinations of pump powers and frequencies where amplification occurs are observed.
In a following measurement the pump frequency and power is fixed and the signal amplification in dependence of the signal frequency is measured. One such measurement is showed in figure 3.4. In this measurement the pump power was fixed at -11.3 dBm, the pump frequency was 6.1441 GHz and the power of the input signal -44 dBm. The data shows the expected shape of a Lorenz function:

$$f(x) = \frac{A \cdot Q_e^2}{4Q_e^4 \cdot \frac{(\omega_0 - x)^2}{\omega_0^2} + Q_e^2} \tag{3.1}$$

Where A corresponds to the maximal amplitude, Q_e to the external quality factor which determines the with of the function and ω_0 is the central frequency. A fit to the Lorenz function in formula 3.1 is performed and given in figure 3.4 in purple. From this fit also the characteristic gain bandwidth product can be calculated. The gain bandwidth product is defined as:

$$\text{GBP} = \frac{\sqrt{A}\omega_0}{Q_e} \tag{3.2}$$

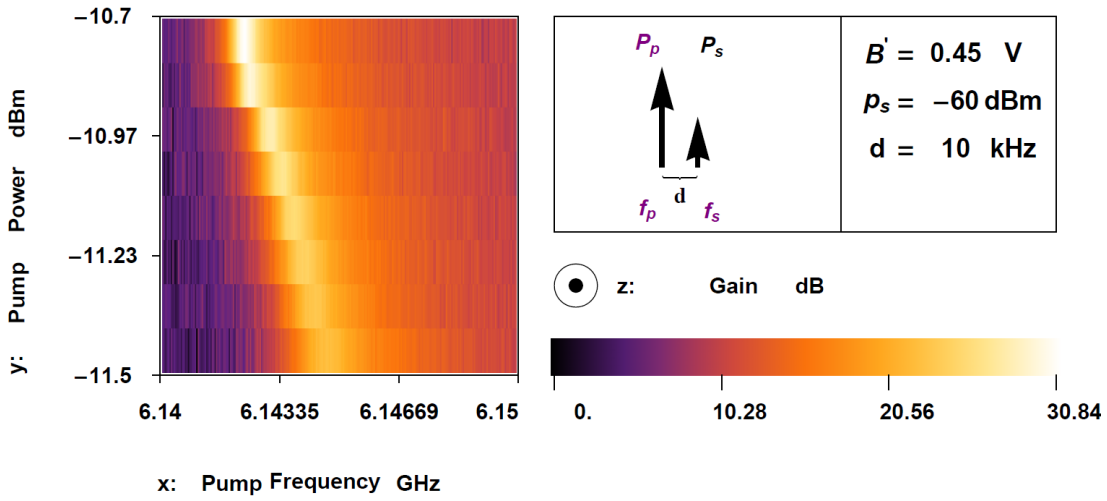

Figure 3.3: ***Single pump gain measurement****: investigation of pump parameters for signal amplification, given as density plot is the signal gain in dependence of the pump parameters, the measurement technique is showed as pictograph where the constant parameters are indicated on the right*

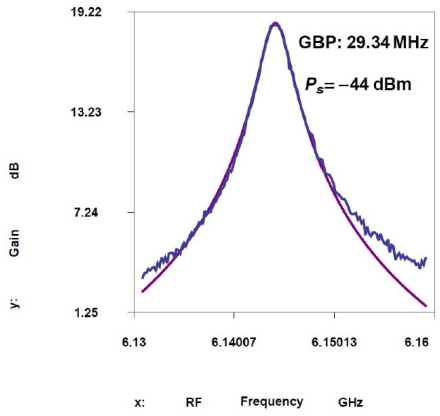

Figure 3.4: ***Signal amplification with one pump drive****: The amplification shows the typical Lorenz shape with a GBP of 29. MHz, data is plotted in blue while a fit to the Lorenz function is given in purple, the pump power is fixed to -11.3 dBm while the pump frequency is 6.1441 GHz*

Now qualitatively the same thing is tested with two pump drives. Amplification is analyzed in dependence of the pump parameters. Where the additional generator yields now two additional degrees of freedom which result in a multiple of possible sweeping techniques. Nevertheless a good amplification point to fix the pump drives was found:

Pump power 1	−14	dBm
Pump frequency 1	6.108	GHz
Pump power 2	−9.8	dBm
Pump frequency 2	6.158	GHz
Detuning	40	MHz

With this frequency spacing of the two pump drives at 40 MHz a gain bandwidth product of 24.55 MHz is achieved. The measurement is given in figure 3.5 in blue the measurement data is shown and again a fit to the Lorenz function is given in purple. Once more the typical Lorenz shape is observed.
Thus it is possible to realize the double pump amplifier to observe expected amplification characteristics which are similar to the single pump amplification.

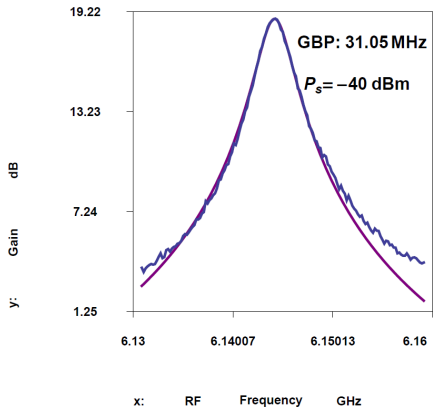

Figure 3.5: ***Signal amplification with two pump drives****: Again the amplification shows the typical Lorenz shape now with a GBP of 24.55 MHz, data is plotted in blue while a fit to the Lorenz function is given in purple, the pump powers are fixed to -14 dBm and -9.8 dBm while the frequencies where 6.108 GHz and 6.158 GHz*

3.3 Test of phasesensitive amplification

In section 2.1 about the advantages of the double pump amplifier the phasesensitive amplification was named as possible field for further applications. In the measurements above the advantage named in 2.1 did not show its benefit. The pump powers where simply averaged out by the measurement technique. A test whether phasesensitive amplification with two pump drives in general works is the next goal.
To observe this the two pump drives are fixed as well as the signal frequency and power. The only parameter which is varied is the signals phase. The measurement is presented in figure 3.6 the pumps are fixed as in the table above. In figure 3.6 one can observe a strong dependence of the amplification on the phase which gives a positive feedback to our test.

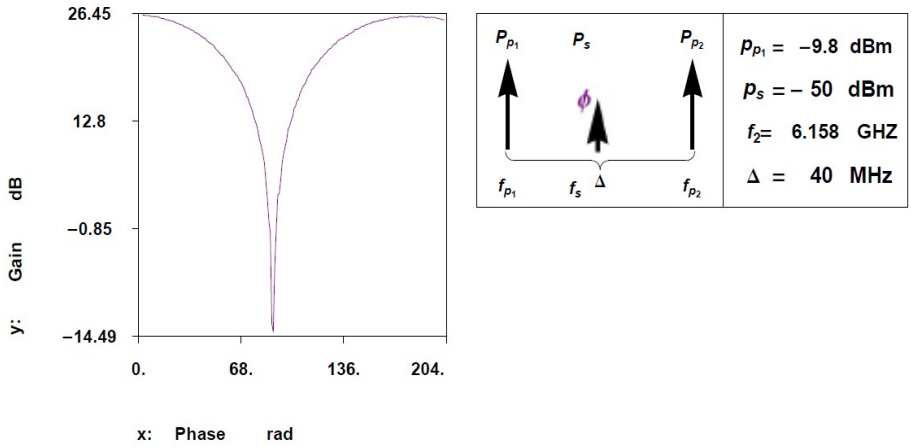

Figure 3.6: ***Gain in dependence of the phase between signal and idler****: Pump powers and frequencies are fixed to the values given in the graphic as well as the signal power and frequency is fixed. Amplification in dependence of the phase is observed*

3.4 Amplification independence of the detuning

Until now it was possible to realize the double pump amplifier and to show its proper operation. With this knowledge one can turn to further aspects of the double pump amplifier. While amplifying with two pump drives the frequencies of the pumps are always separated by a certain amount (detuning). When testing the double pump amplifier several questions arose: How does the amplification depend on this detuning? Is it possible to change steadily from double pump to single pump amplification by decreasing the detuning to zero?
A difficulty in the measurement technique where frequency dependent losses in the setup. Because the two pumps are at different frequencies the cables and attenuators do not absorb the same way at both values. This makes it difficult to achieve the same pump strength of both pumps at the sample. How sensitive is the amplification process to such asymmetries in pump strength?

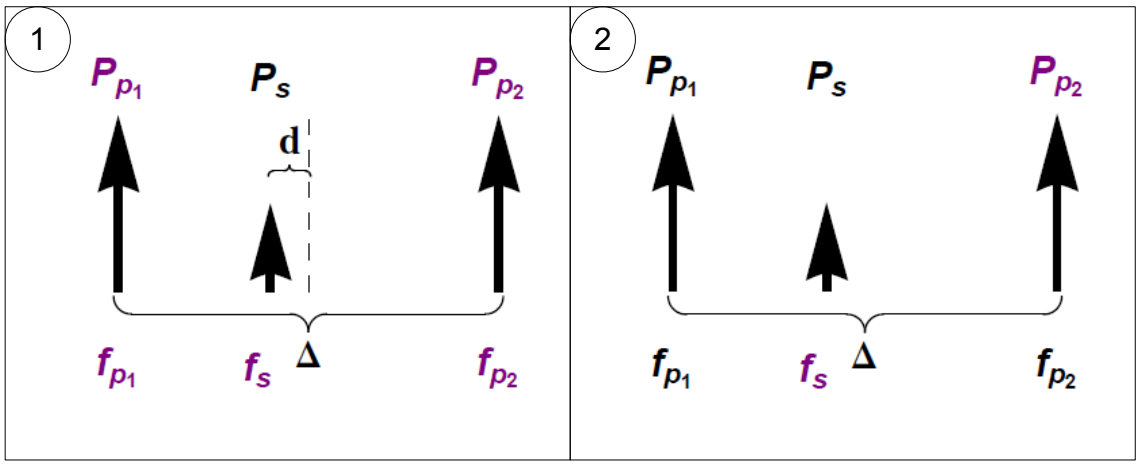

Figure 3.7: ***Measurement technique****: First measurement all frequencies have the same detuning to each other, the signal is 10 kHz away from the center, All three frequencies are swept together,in addition the two pump strength are varied simultaneously; Second measurement the two pump frequencies and one pump power are fixed , varied are the signals frequency as well as the second pump power*

To answer this questions experimentally first a measurement technique is developed and defined. Most useful proved the two measurements shown in figure 3.7. In a first measurement the characteristics of good pump drives is searched. To do so all three frequencies have the same detuning to each other and are varied simultaneously. The signal is 10 kHz away from the center. While sweeping the frequencies the two pump powers are changed in the same way. This measurement is somehow analogue to the one shown in figure 3.3. In a second step the pump drives are fixed and only the signals frequency is varied. But in contrast to earlier measurement only one pump power is fixed the other one is swept. This gives the possibility to observe how sensitive the amplification depends on inequalities of the input power.
This two measurements were performed with several different detunings. In figure 3.8 the measurement with a detuning of 4 MHz is presented. The top picture shows the results from the first measurement. Amplification is observed on a diagonal looking similar to the measurement in figure 3.3. Below a picture of the second measurement is found. The power region were amplification is observed is about 0.8 dBm. One scan from this measurement should again give a Lorenz curve. This is shown in the bottom picture. No Lorenz curve is observed in this picture.
The measurements were also performed with 60 MHz of detuning. The results are given in figure 3.9. Here the first measurement does not show similarities to figure 3.3. In the second picture it is seen that amplification occurs now over a region of 3 - 4 dBm. Which can eventually be explained by a smaller percentage of power coupling into the resonator. Because the pump is detuned more from the resonance frequency. One scan of measurement 2 looks like a Lorenz curve.
In total it was observed that for high detunings the first measurement gave results which were difficult to interpret. But when once the pump was fixed it was possible to observe Lorenz curves. Also the power region of the second pump were amplification occurred increased with the detuning. At small detunings the first measurement gave always a picture of a "long diagonal". While power regions were small and it was really hard to tune the experimental setup such that Lorenz curves could be observed.

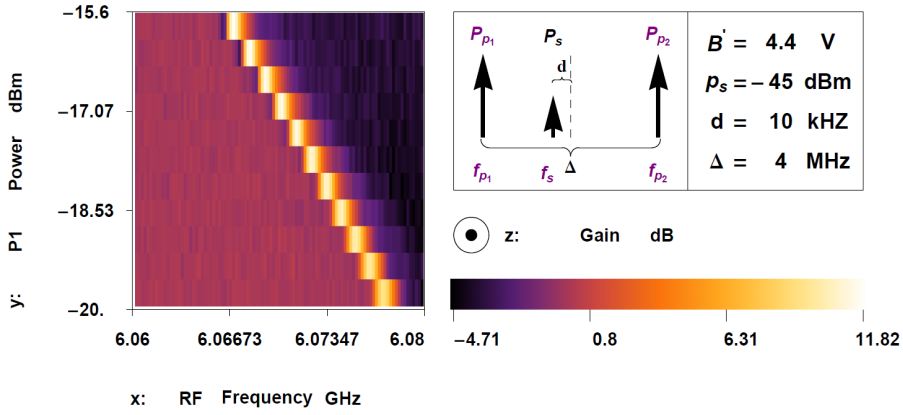

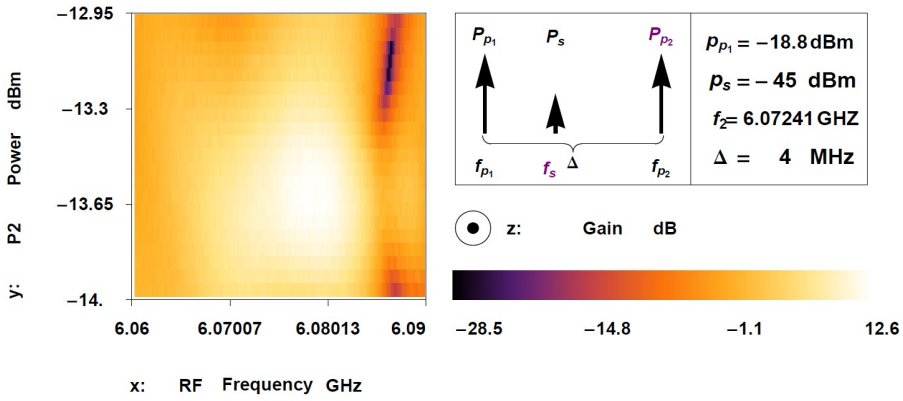

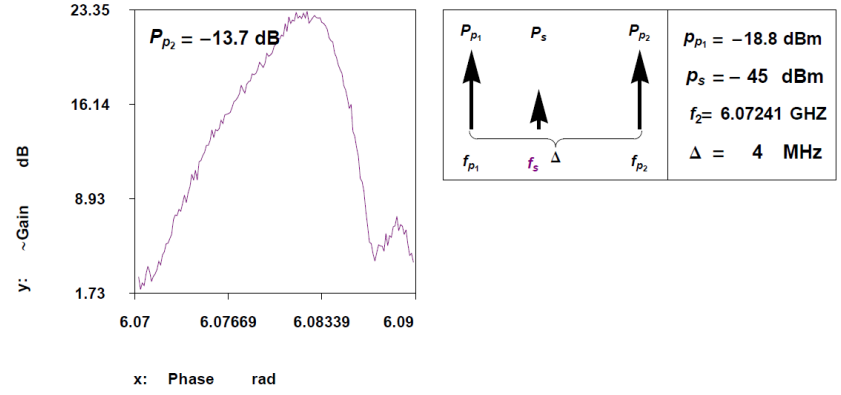

Figure 3.8: ***Detuning of 4 MHz****: Top picture mes 1: Amplification on a diagonal, middle mes 2: Region of 0.8 dBm were amplification occurs, bottom one scan of mes 2: does not show a Lorenz curve*

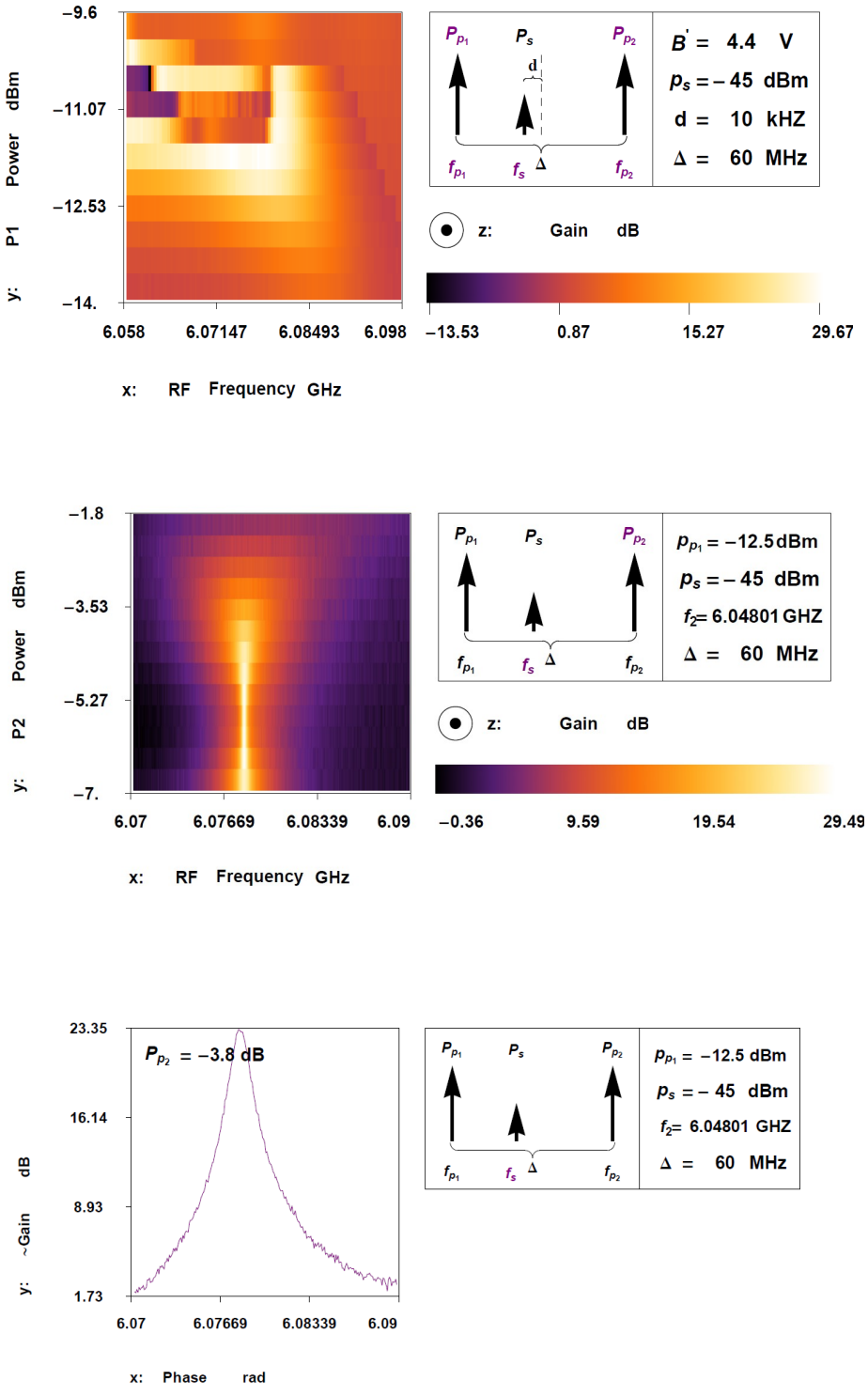

Figure 3.9: ***Detuning of 60 MHz****: top picture mes 1: Difficult to interpret, middle mes 2: Region of 3 - 4 dBm were amplification occurs, bottom one scan of mes 2: shows a Lorenz curve*

Chapter 4

Conclusion and outlook

It was possible to realize the double pump amplifier and produce similar amplification as in the single pump case. Also phase sensitive amplification was tested with two pump drives and showed positive results. To further analyze the double pump and the amplification in dependence of the detuning a measurement technique was developed. To sweep all frequencies simultaneously and with constant frequency spacing seemed most convenient as starting point. In a second measurement the frequencies of the two pump drives are fixed. In contrast to the single pump case only one pump power is fixed. This seemed reasonable to explore the effects of the individual pump drive powers. The amplification was examined in dependence of different constant detunings. It was found that the first measurement showed more expected behavior for small detunings. But it was difficult to fix the pump drives to achieve nice signal gain curves. The power region where the amplification in the second measurement occurred increased for bigger detunings. As well as the overall pump strength. Both effects were explained by the fact that less power couples into the resonator for bigger detunings.
In the extent of a semester project the double pump amplifier was studied and some of its characteristics were measured. The next step in analysis of the double pump amplifier would be to confirm first the results found in this project and then to enlarge them. Interesting points to measure are for example the boarder between double pump amplification and single pump amplification. It would be instructive to show that it is possible to change steadily from the double pump to the single pump by decreasing the detuning. Also the difficulties with the different pump strength should be analyzed further and the amount of power coupling into the resonator at a particular detuning should be compared with the expectations. There are also more delicate aspect which could be analyzed. The soft pump regime as discussed in [2] could be explored. When all characteristics and advantages of the double pump amplifier are known, then one could decide weather an additional generator is worth to do amplification.

Appendix A

Basic model of the parametric amplifier

The whole microwave resonator system can be described by a parallel LRC-circuit with a non-linear inductance. Such a circuit can be described by a differential equation with only one degree of freedom, the node flux. This variable is defined as the sum of branch fluxes connecting the node with the defined ground node. One such branch flux is the integral over the time since $-\infty$ of the instantaneous flux through the branch. For more details to the exact definition and the derivation of such an differential equation see the text [3]. The differential equation for the circuit in figure 2.5 is given by:

$$\ddot{\Phi} + 2\Gamma\dot{\Phi} + \omega_0^2(1 + \lambda(\frac{2\pi\Phi}{\Phi_0})^2) = \frac{1}{C}(I_{RF1}\cos(\omega_1 t) + I_{RF2}\cos(\omega_2 t) + I_N)[2] \tag{A.1}$$

The second term describes the decay in the resonator with the damping constant Γ as characterisitc parameter. The nonlinearity is put into the formula via the nonlinearity coefficent λ. For a SQUID this constant is $\lambda = \frac{1}{6}$. With the help of this constant the formula can be extended to different non linearity as for example an array of SQUIDS as in our case. Then there are two terms describing the pump drives with strengths I_{RF1}, I_{RF2} and frequencies ω_1 and ω_2. The last term considers the input signal.

To sum up the different parameters in the equation are:

Φ	: node Flux	(A.2)
I_{RF1}, I_{RF2}	: pump drives	
I_N	: Incoherent signal input	
$\Gamma = \frac{1}{RC}$	: Damping constant	
$\omega_0 = \frac{1}{\sqrt{L_j C}}$	: natural resonance frequency	
λ	: non linearity coefficient	
$L_j = \frac{\hbar}{2eI_0}$	: linear Inductance	
$\delta L_j = \lambda L_j I^2 / I_0^2$	: non linear inductance	

Equation A.2: **Summary of the relevant quantities**

The differential equation is changed to dimensionless coordinates with the substitution $\phi = 2\pi\Phi/\Phi_0$ and $\nu^{in} = I_N R 2\pi/\Phi_0$.

$$\ddot{\phi} + 2\Gamma\dot{\phi} + \omega_0^2\phi(1+\lambda\phi^2) - \omega_0^2\frac{I_{RF1}^2}{I_0^2}\cos(\omega_1 t) + \omega_0^2\frac{I_{RF1}^2}{I_0^2}\cos(\omega_2 t) = 2\lambda\nu^{in}) \tag{A.3}$$

Equation A.3: **Dimensionless DGL**

This differential equation is approximately solved with an appropriate ansatz given in formula A.4. The solution can contain all possible frequencies this is given in the first term of the ansatz. It contains noise as well as the signal and the idler. In the stiff pump approximation where pumping with high power is assumed, ω_1 and ω_2 as well as the possible self-oscillation frequency $\omega_g = \frac{\omega_1+\omega_2}{2}$ are the dominant frequencies of the system. $\chi[\omega]$,Y,Z,Ξ are the coefficients of the different frequencies.

$$\varphi(t) = \int_{-\infty}^{\infty}\chi[\omega]e^{-i\omega t}\,\mathrm{d}\omega + \Xi e^{-i\omega_g t} + Ye^{-i\omega_1 t} + Ze^{-i\omega_g t} + c.c. \tag{A.4}$$

Equation A.4: **Ansatz**, c.c. refers to the complex conjugated terms

Useful for a clear calculation is also the quantity given in formula A.5. This term shows the depletion of the pump drives via the internal coupling which can be seen from formula A.7. This is why Π is usually refereed to as back action factor.

$$\Pi = \left\langle \int_{-\infty}^{\infty}\int_{-\infty}^{\infty}\chi[\omega_a]\chi[\omega_b]\,\mathrm{d}\omega_a\,\mathrm{d}\omega_b\delta(\omega_a+\omega_b+2\omega_g)\right\rangle \tag{A.5}$$

Equation A.5: **Back Action Factor**

The basic coupling between the internal coordinates are given by:

$$\omega_I = 2\omega_g - \omega_s \qquad \text{where } \omega_g = \frac{\omega_1 + \omega_2}{2} \tag{A.6}$$

Equation A.6: **Coupling of the frequencies**

Now the ansatz is inserted into the differential equation and harmonic balance for $\omega_s, \omega_I, \omega_g, \omega_1$ and ω_2 is performed. This means the coefficients before the exponential term for one frequency are equated. In doing harmonic balance also several approximations are performed: All fast oscillations are neglected (e.g. $2\omega_1$), Y and Z are considered to be much bigger than the other coefficients especially Π and terms only performing a re normalization are disregarded. To perform this calculation φ^3 has to be calculated. This is done in equation A.7. Together with the other terms in the dimensionless DGL and in performing harmonic balance a system of 10 equations is obtained.

$$\begin{aligned}
\varphi^3 = \quad & + e^{-i\omega_s t} && (\chi[\omega_s](3\chi[\omega_s]\chi[\omega_{-s}] + 6\chi[\omega_I]\chi[\omega_{-I}] + 6\Xi\Xi^* + 6YY^* \\
& & & + 6ZZ^*) + 6\chi[-\omega_I]YZ + 6\Pi\chi^*[\omega_I] + 6\chi^*[\omega_I]\chi^2) \\
& + e^{-i\omega_I t} && \chi[\omega_I](3\chi[\omega_I]\chi[\omega_{-I}] + 6\chi[\omega_s]\chi[\omega_{-s}] + 6\Xi\Xi^* + 6YY^* \\
& & & + 6ZZ^*) + 6\chi[-\omega_s]YZ + 6\Pi\chi^*[\omega_s] + 6\chi^*[\omega_s]\chi^2) \\
& + e^{-i\omega_g t} && (\Xi(6\chi[\omega_s]\chi[\omega_{-s}] + 6\chi[\omega_I]\chi[\omega_{-I}] + 3\Xi\Xi^* + 6YY^* \\
& & & + 6ZZ^*) + 6\Xi^*YZ + 6\Xi^*\chi[\omega_s]\chi[\omega_I] \\
& + e^{-i\omega_2 t} && (Z(6\chi[\omega_s]\chi[\omega_{-s}] + 6\chi[\omega_I]\chi[\omega_{-I}] + 6\Xi\Xi^* + 6YY^* \\
& & & + 3ZZ^*) + 6\Pi Y^* + 3\Xi^2 Y^* \\
& + e^{-i\omega_1 t} && (Z(6\chi[\omega_s]\chi[\omega_{-s}] + 6\chi[\omega_I]\chi[\omega_{-I}] + 6\Xi\Xi^* + 3YY^* \\
& & & + 6ZZ^*) + 6\Pi Z^* + 3\Xi^2 Z^* \\
& + c.c. \\
& + f.o.
\end{aligned} \tag{A.7}$$

$$\begin{aligned}
\varphi^3 \approx \quad & + e^{-i\omega_s t} && 6\chi[-\omega_I]YZ \\
& + e^{-i\omega_I t} && 6\chi[-\omega_s]YZ \\
& + e^{-i\omega_g t} && 6\Xi^*YZ \\
& + e^{-i\omega_2 t} && 6\Pi Y^* + 3\Xi^2 Y^* \\
& + e^{-i\omega_1 t} && 6\Pi Z^* + 3\Xi^2 Z^* \\
& + c.c.
\end{aligned}$$

Equation A.7: **Calculation and approximation of** φ^3, f.o.: fast oscillating terms

$$(-\omega_s^2 - 2i\Gamma\omega_s + \omega_0^2)\chi[\omega_s] + \lambda\omega_0^2(6\chi[-\omega_I]YZ) = 2\Gamma\nu^{in}[\omega_s] \tag{A.8}$$
$$(-\omega_I^2 - 2i\Gamma\omega_I + \omega_0^2)\chi[\omega_I] + \lambda\omega_0^2(6\chi[-\omega_s]YZ) = 2\Gamma\nu^{in}[\omega_I] \tag{A.9}$$
$$(-\omega_1^2 - 2i\Gamma\omega_1 + \omega_0^2)Y + \lambda\omega_0^2(6\Pi Z^* + 3\Xi^2 Z^*) = \frac{\omega_0^2 I_{RF1}}{2I_0} \tag{A.10}$$
$$(-\omega_2^2 - 2i\Gamma\omega_2 + \omega_0^2)Y + \lambda\omega_0^2(6\Pi Y^* + 3\Xi^2 Y^*) = \frac{\omega_0^2 I_{RF2}}{2I_0} \tag{A.11}$$
$$(-\omega_g^2 - 2i\Gamma\omega_g + \omega_0^2)\Xi + \lambda\omega_0^2(6\Xi^* YZ) = 0 \tag{A.12}$$
c.c.

Equation A.8-A.12: **System of equations**

Equation A.10 and A.11 and the corresponding c.c. equations are solved for the product YZ. To do this calculation the high Q limit is assumed ($\Gamma \ll$ Q). In addition only terms linear in λ are considered (weak non linear limit). To make the approximate result more readable the quantities γ and $\widetilde{f_i}$ are defined.

$$\begin{aligned}\gamma &= \frac{2\lambda}{(1+\frac{\omega_1}{\omega_0})(1+\frac{\omega_2}{\omega_0})} \\ \widetilde{f_i} &= \frac{I_{RF_i}}{I_0(1+\frac{\omega_i}{\omega_0})|1-\frac{\omega_i}{\omega_0}|} \\ \mathrm{YZ} &= \widetilde{f_1}\widetilde{f_2}(-1+\gamma(\Pi+\frac{1}{2}\Xi^2)\end{aligned} \tag{A.13}$$

Equation A.13: **Pump strength and back action**

The $\widetilde{f_i}$ are essentially the pump strength and γ the renormalized non linearity. In formula A.13 it is seen that the effect of back action onto the coefficients YZ depends on the parameter λ. In the double pump analysis only the product of YZ is important not the individual parameters. To analyse signal and idler gain a even stronger approximation is done. Equation A.13 then becomes simply:

$$\mathrm{YZ} = -\widetilde{f_1}\widetilde{f_2} \tag{A.14}$$

Equation A.14: **Pump under stiff pump approximation**

Now the approximated product YZ is inserted into equation A.11 and A.12 and the corresponding c.c. equation. The variables are changed to reduced de tunings: $\Delta = \frac{\omega_s-\omega_g}{\Gamma}$, $\Omega = \frac{\omega_0-\omega_g}{\Gamma}$. The equation are rearranged under the assumption $\omega_0 \approx \omega_s$. A system of 4 linear equations for the coefficients χ is obtained.:

$$\begin{pmatrix} \Omega-\Delta-2i & 0 & 0 & -F \\ 0 & \Omega+\Delta-2i & -F & 0 \\ 0 & -F & \Omega-\Delta+2i & 0 \\ -F & 0 & 0 & \Omega+\Delta+2i \end{pmatrix} = \frac{2}{\omega_0}\begin{pmatrix} \chi[\omega_s] \\ \chi[\omega_I] \\ \chi[-\omega_s] \\ \chi[-\omega_I] \end{pmatrix} \tag{A.15}$$

Equation A.15: **Linear system of equations for χ coefficients**

Where the abbreviation F is: $F = \frac{\widetilde{f_1}\widetilde{f_2}6\lambda\omega_0}{\Gamma}$. This system can now easily be solved for the χ coefficients. The χ coefficient describe the internal variables of the system. With the help of input-output theory the relation between input and output field can be found:

$$\hat{a}^{out}[\omega] = i\chi[\omega] - \hat{a}^{in}[\omega] \tag{A.16}$$

Equation A.16: **Input output theory**

From this calculation the output of a measurement in dependence of the different input variables can be calculated and predicted.

Appendix B

Additional measurement results

B.1 Sample 1: Tunability and quality factor

The analysis of the double pump amplifier started with a first sample. But in few measurements it was clear that this sample did not have the designed properties. Especially the external quality factor was much lower than the sample was designed for. Thus only few measurements were performed and a second sample was produced. Nevertheless some results with this sample 1 are shown here.
The analogue measurement as presented in section 3.1 was performed also with sample 1. The results are shown in figure B.1: the blue dots show the resonance frequencies extracted from the reflection coefficient measurements and the red line is a fit to the theoretical calculation. There occur several small local maxima. The first one occur because the flux through the array of SQUIDs is not homogeneous. This was neglected in the description of the SQUID array with one inductance.
From this measurement the external quality factor is calculated, see figure B.2. From figure B.2 one can conclude, that the quality factor is higher for lower resonance frequencies. Hence the expectation is to observe a more predictable amplification behavior for lower frequencies.

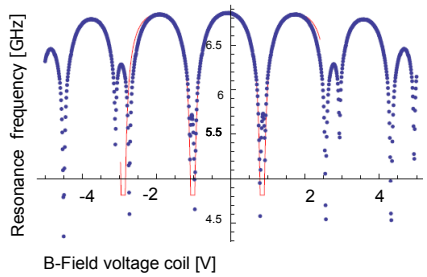

Figure B.1: ***Resonance frequency dependence on the flux through the SQUIDs*** *Blue: Measurement, Red: Fit*

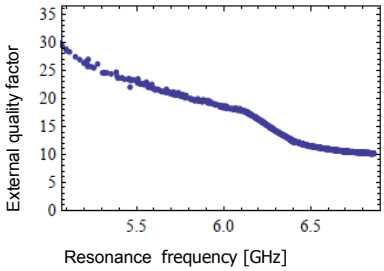

Figure B.2: ***External Quality factor for different resonance frequencies***

B.2 Sample 1: Single pump measurements

To analyse sample 1 a collection of measurements analogue to the measurement in figure 3.3 were performed. Each measurement differes in the voltage on the coil meaning the resonance frequency. They are presented in figure B.3. For a quite high resonance frequency as in the top picture the domain where amplification occurs is not well understood. This is as expected because the quality factor is lower for higher resonance frequencies. The pictures become clearer for higher B-fields. Nevertheless they have still sharp bends which are not understood. The last picture which is again stranger already belongs to the next maxima in figure B.1.
An optimal pump frequency and power is searched. A good working point is found for a B-field of 0.87 V and a power of -9.6 dBm. The signal gain for different frequencies is measured 10 times. All curves are shown in figure B.4.
The measurement is stable all curves lie nearly over each other. The curves have also the typical lorenz shape as it should be. The ideal frequency is read out to be 5.54861 GHz. Now the pump is fixed and the signal power and frequency is swept. A density plot is shown in figure B.5. Then the measurement data from one scan is fit to a Lorenz function. From the fit parameters the GBP is calculated. Here four different scans are shown with the corresponding fits to Lorentz curves.

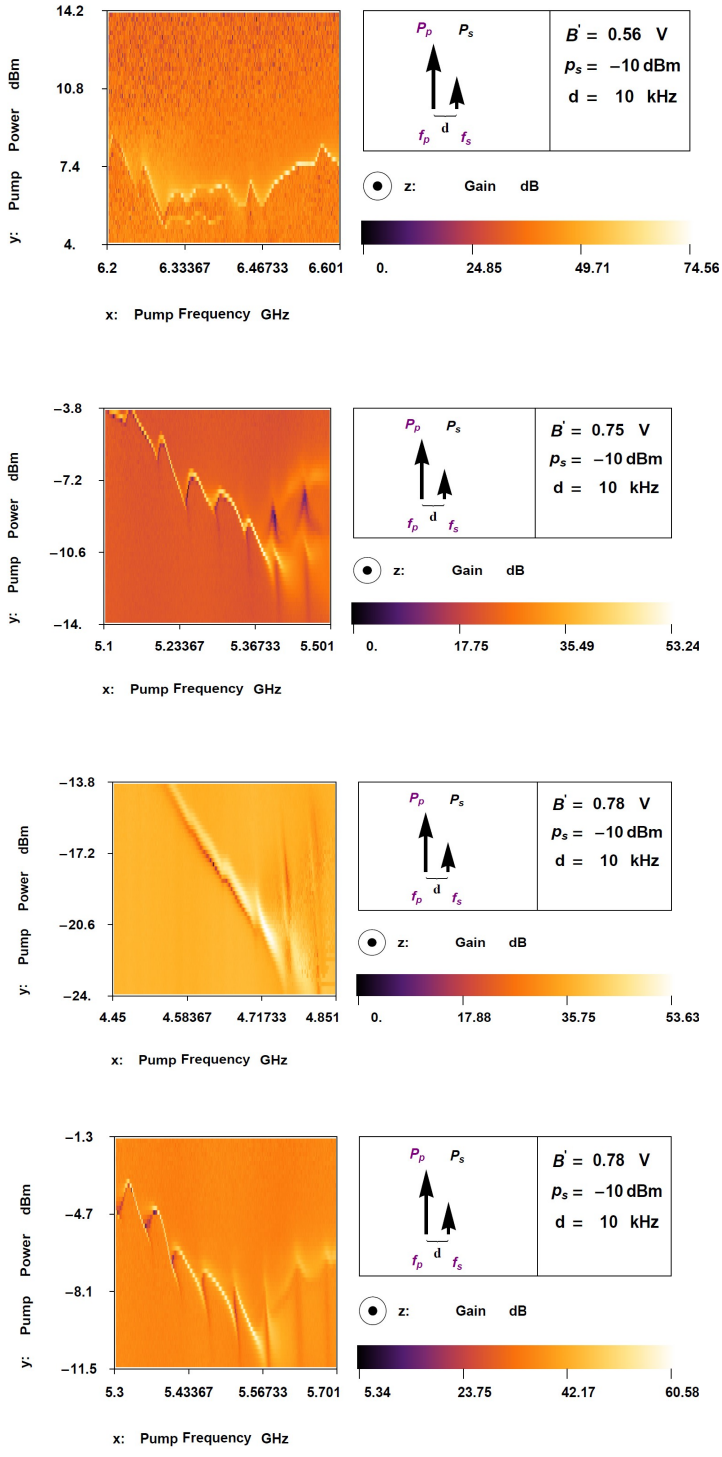

Figure B.3: ***Gain Measurement with different resonance frequency****: Resonance frequency decreases from top to bottom*

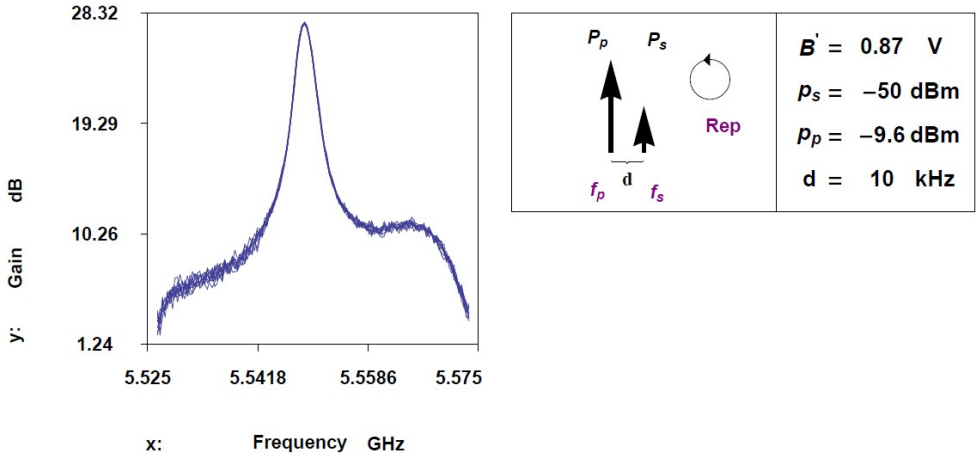

Figure B.4: *Repetition measurement to find pump frequency*

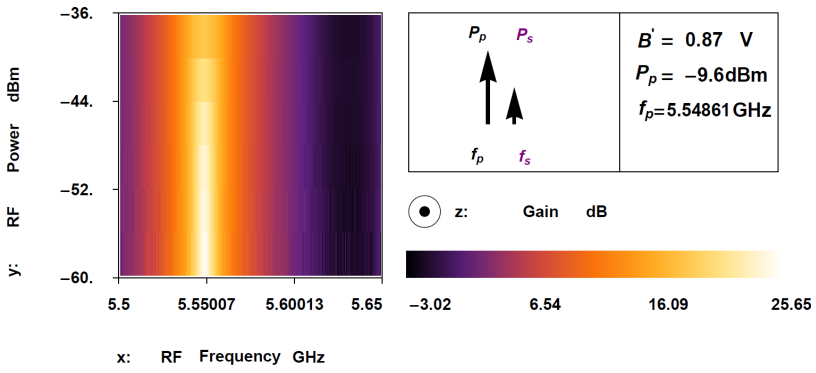

Figure B.5: *Fixed single pump, signal gain*

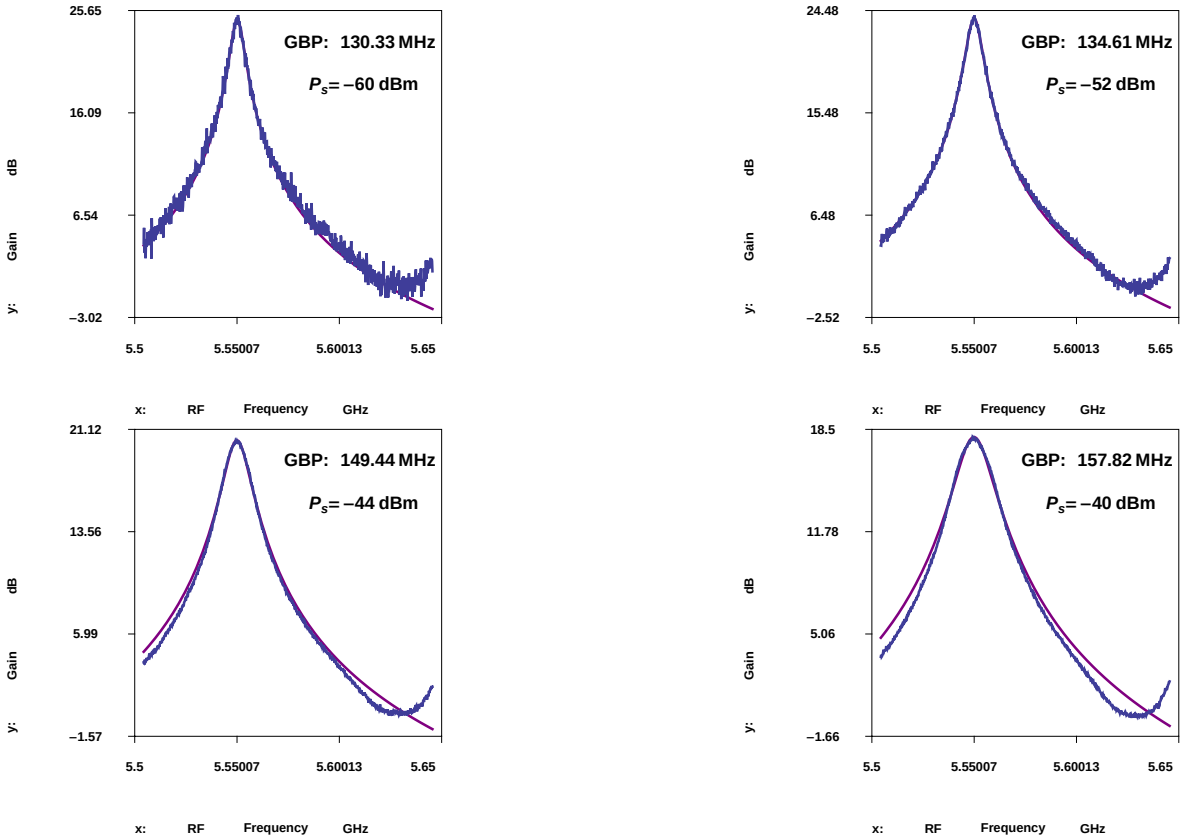

Figure B.6: *Fixed single pump, signal gain fitted to Lorentz function and GBP calculation*

B.3 Sample 1: Double pump measurements

To get a first overview the signal frequency is fixed at 10 kHz de tuned from the already found resonance frequency. The two pump frequencies lie symmetric about this resonance frequency and are swept simultaneously with growing distance. While the difference in pump powers is kept constant at 4dB. The result from this measurement is shown in figure B.7.
First it is seen that the picture is symmetric this should be the case because if the roles of the generators are changed the situation is the same. When the distance from the pump to the signal increases less power couples into the resonator that is why for higher power amplification occurs at more distant frequencies. In the middle there is a lighter narrow band. This occurs because the pump drives does not average out in the right way.

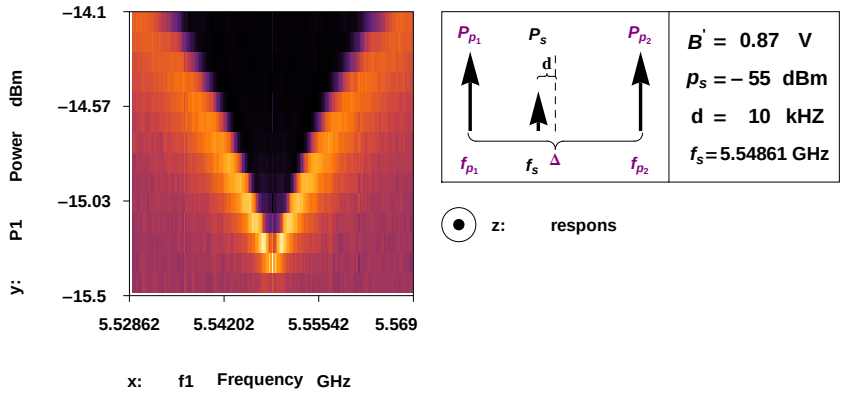

Figure B.7: ***Test of the double pump amplifier***

B.4 Sample 2: Additional measurements

In the following additonal measurement traces to the measurements of section 3.2 are presented. Figures B.8 and B.9 show singel pump measurements. In figures B.10 and B.11 double pump measurements are shown.

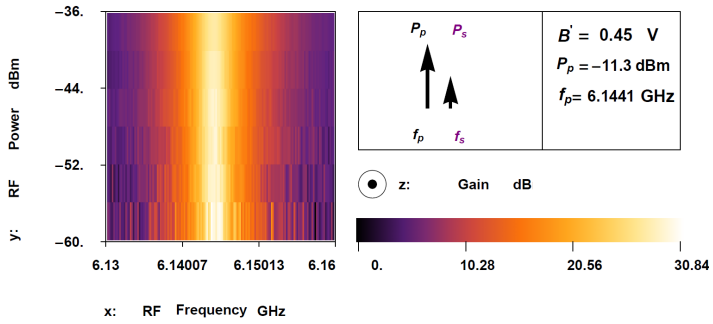

Figure B.8: *Fixed single pump, signal gain*

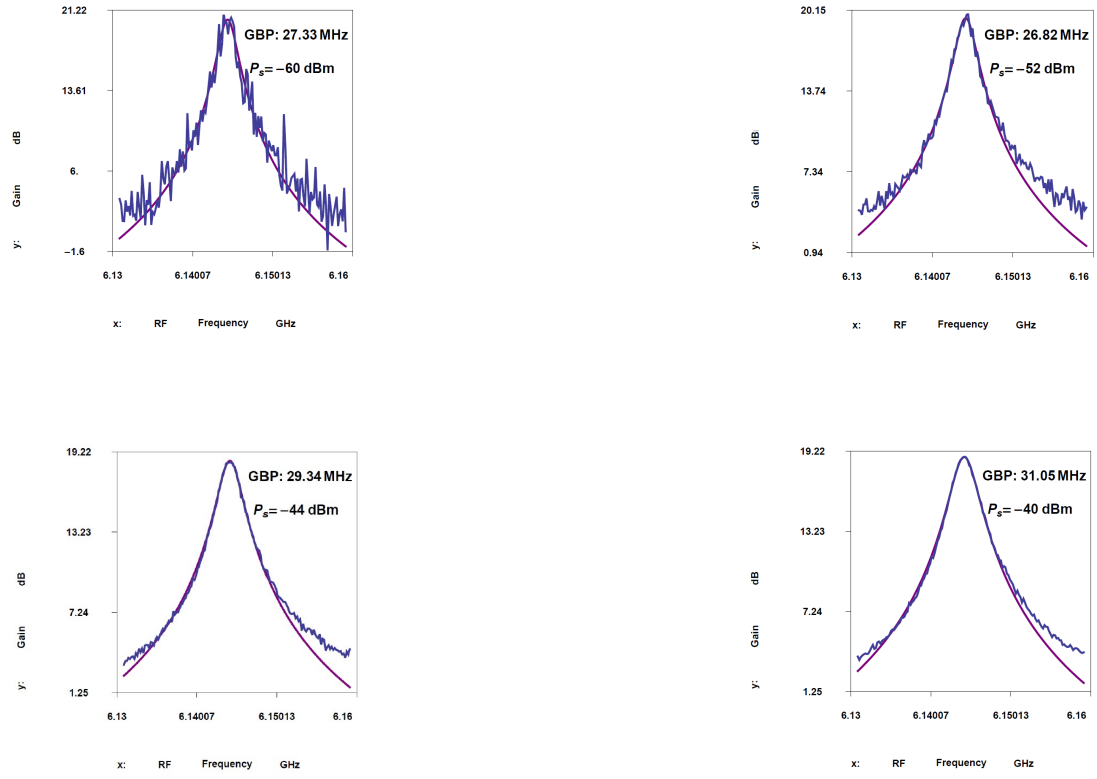

Figure B.9: *Fixed single pump, signal gain fitted to Lorentz function and GBP calculation*

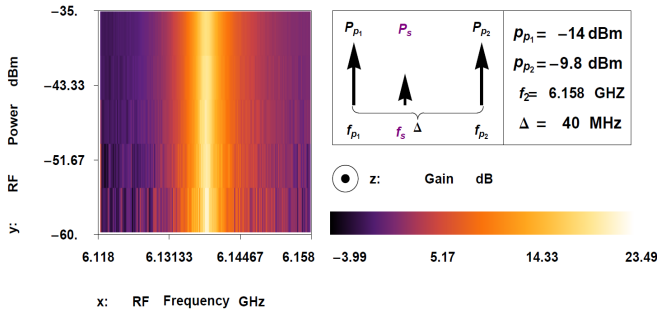

Figure B.10: *Fixed double pump, signal gain*

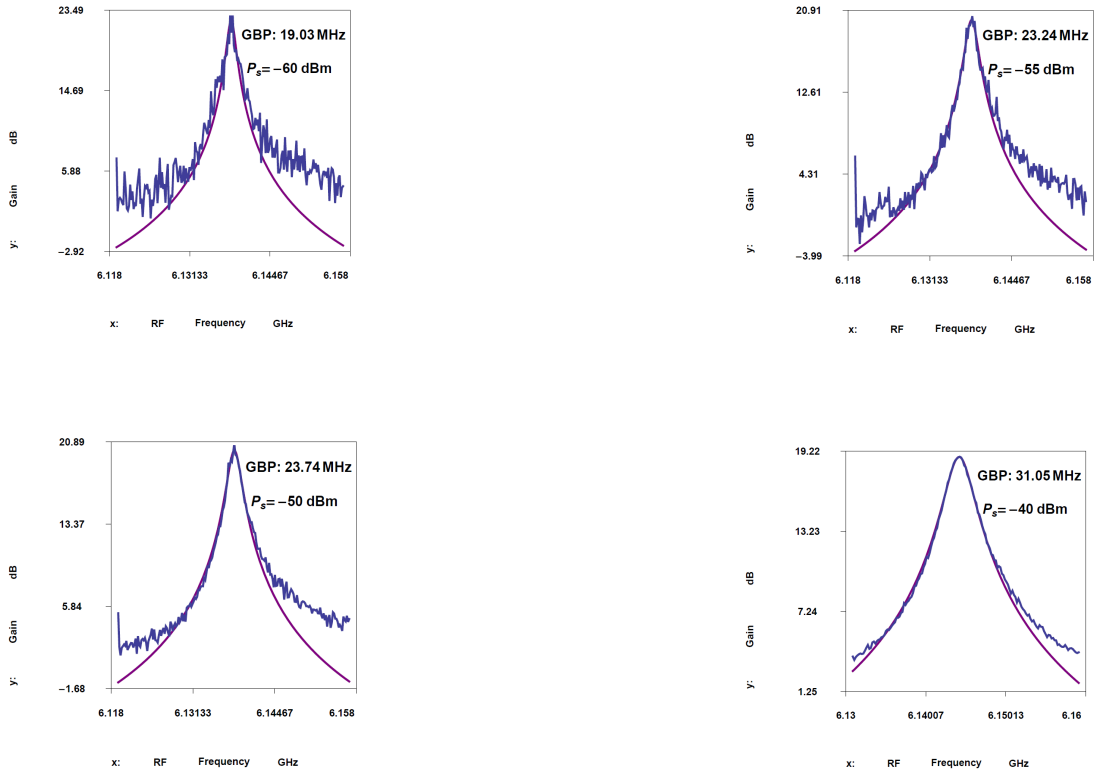

Figure B.11: *Fixed double pump, signal gain fitted to Lorentz function and GBP calculation*

Discussion of the measurement method

To analyze the double pump in a ordered and more extensive way. The first idea was to perform a similar analysis as with sample 1. But the sweeping method with which figure B.7 was obtained soon showed some difficulties and it was necessary to think about better measurements techniques.
Two measurements with the old sweep technique where the signal frequency is held constant while the detuning is increasing linearly and symmetric are shown in figure B.12. The right pictures extends the power region of the left one and looks interesting. The problem with this technique is the fact that if the power coupling into the resonator changes then the resonance frequency changes too. Thus it is not sure that the signal is fixed near the resonance frequency at an optimal position.
The idea is that simultaneous sweeping of all frequencies with constant detunings is a better way. As second parameter both pump powers are swept. For this kind of measurements it is expected that in a certain range there is always one ideal power belonging to one paricular frequency where amplification is strongest. The result of such a measurement is shown in figure B.13. This picture shows that at least in this region the expectation does hold. This kind of measurement also provides a possibility to analyze different constant detunings, which is also an interesting new degree of freedom of the double pump. Also this kind of sweeping is somehow the double pump analog of the gain measurement in the single pump case.
One difficulty with this measurement is to generate exactly the same pump powers with the two generator. This is difficult because the two generators are connected with different cables especially they differ in length. The difference in attenuation because of the cable length can be measured and compensated in the double pump measurement. More complicated is the fact that there also occur frequency dependent loses, which are not explained yet. Thus when the frequency is swept the power difference at the sample of the two generators varies in their size. Thus it is reasonable to fix the two pump frequencies and one pump power and then to sweep the second pump power and the signal frequency. In this measurement the influence of the power difference of the two generators can be seen. In the end the pump can be fixed totally and the signal gain can be analyzed. To sum up a good analysis of the double pump and its different detuning can be the following:

Double pump measurement method

1. simultaneous sweep of the two pump and the signal frequency together with varying pump power.

2. fix pump frequencies and one pump power, sweep signal frequency and second pump power.

3. fix pump, sweep signal power and frequency.

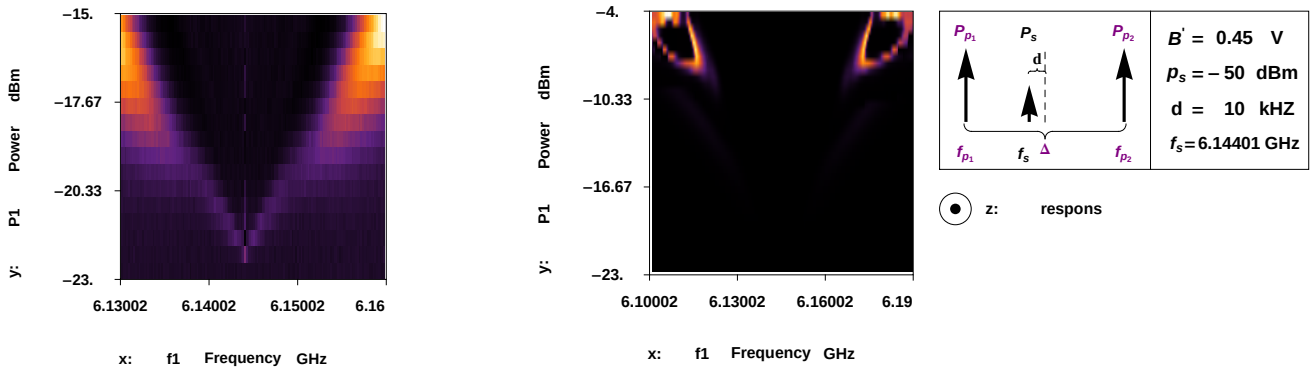

Figure B.12: *Problems with the intuitive sweeping method*

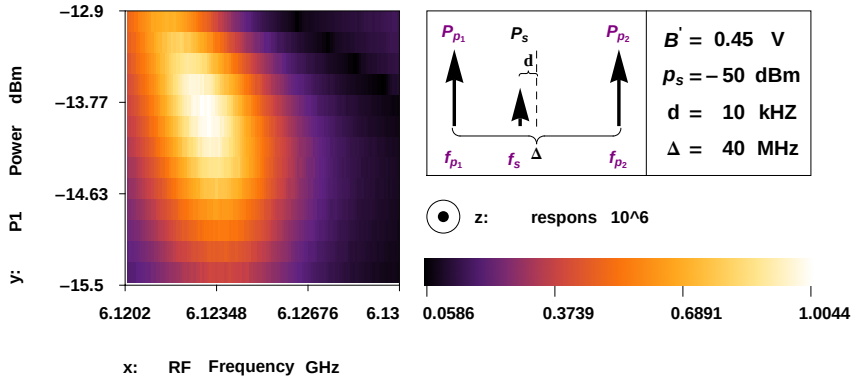

Figure B.13: *New sweeping technique*

Additional Measurement results to Section 3.4

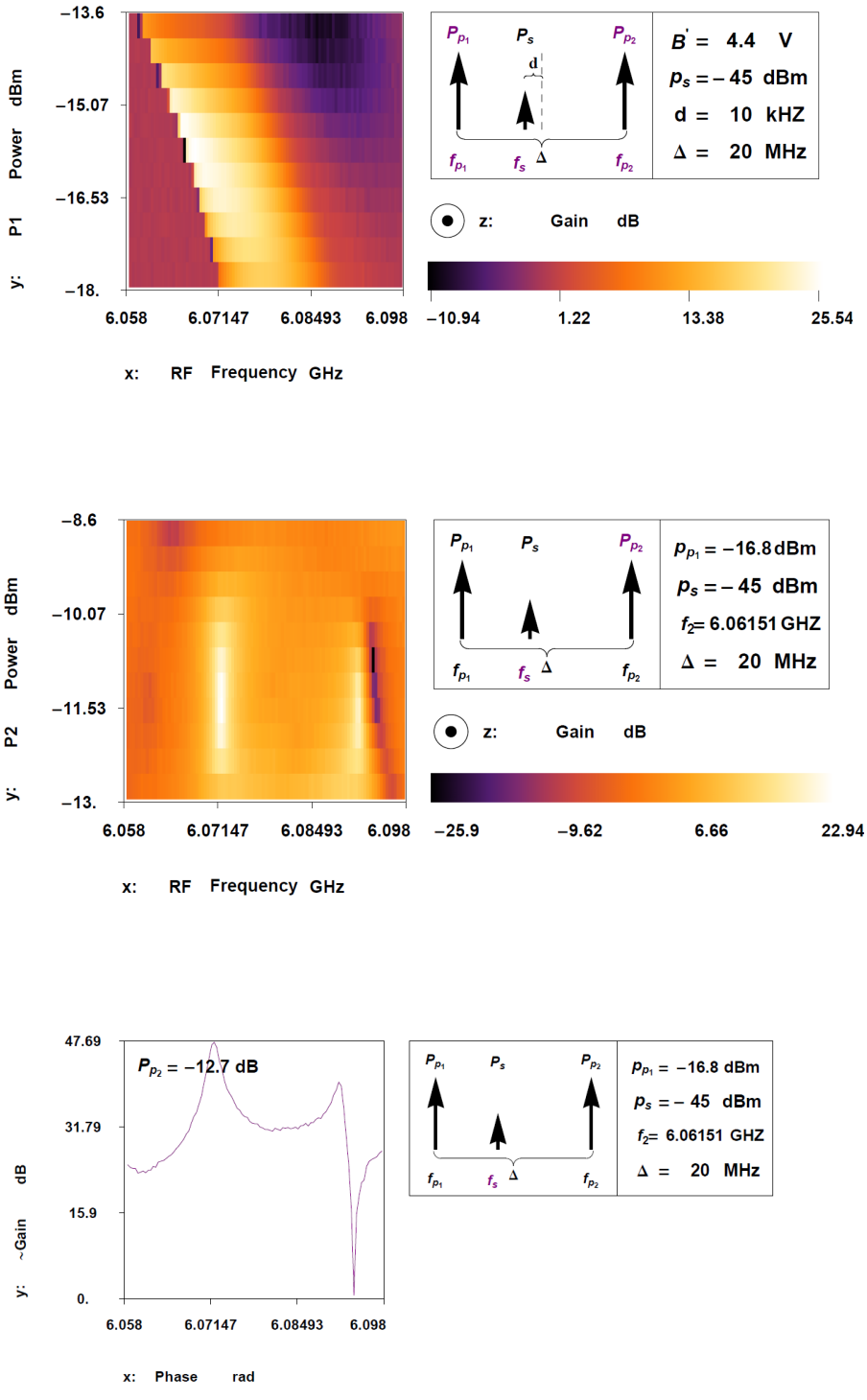

Figure B.14: ***Detuning of 20 MHz****, top picture mes 1, middle mes 2, bottom one scan of mes 2*

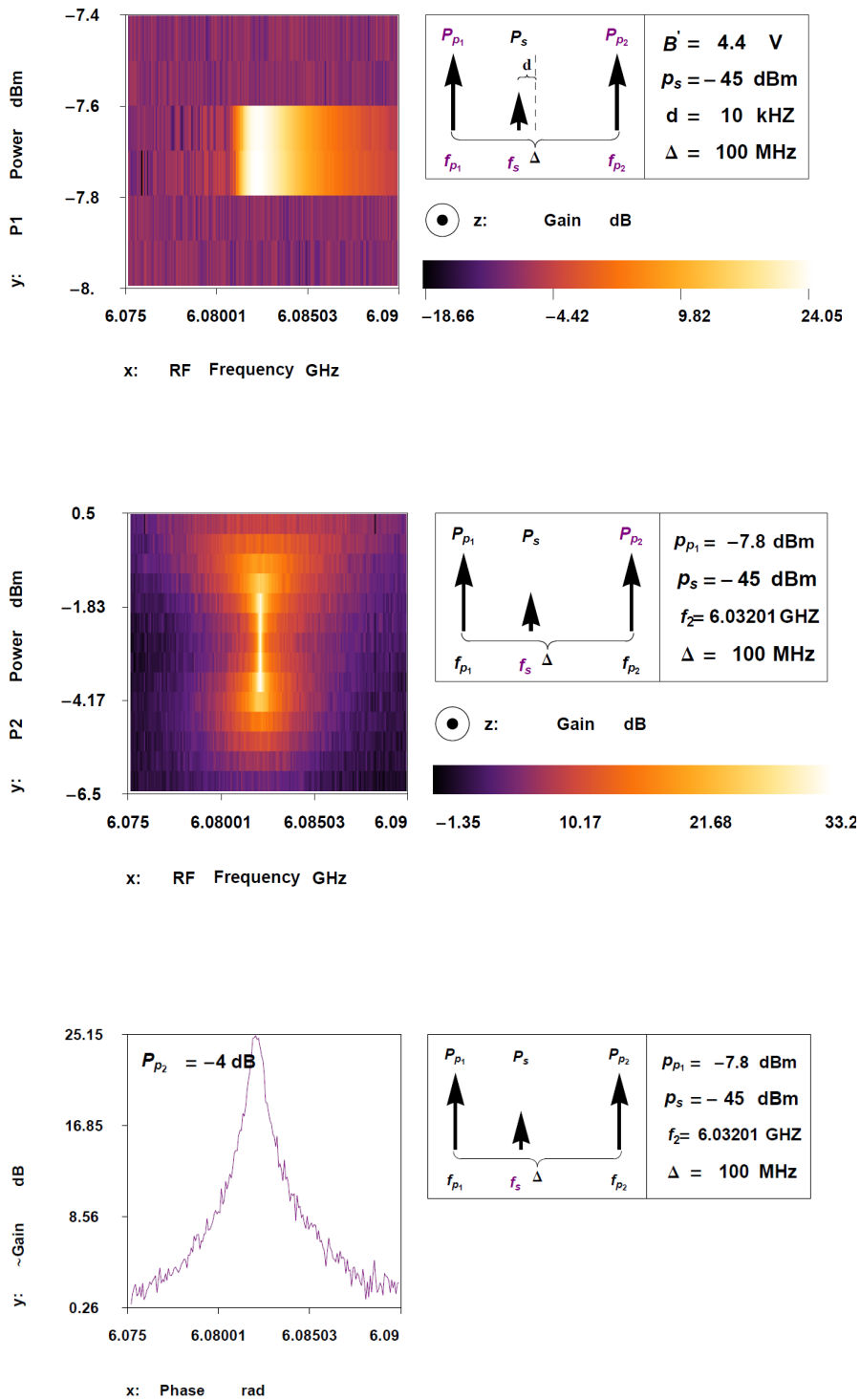

Figure B.15: ***Detuning of 100 MHz****, top picture mes 1, middle mes 2, bottom one scan of mes 2*

Bibliography

[1] A. Blais L. Frunzio R.-S. Huang J. Mayer S. Kumar S.M. Girvin und R. J. Schoelkopf A. Wallraff, D. I. Schuster. Strong coupling of a single photon to a superconducting qubit using circuit quantum electrodynmaics. *Nature*, 431:162–167, 2004.

[2] A.Marblestone A.Kamal and Michel Devoret. Signal-to-pump bakc action and self-oscillation in double-pump josephson parametric amplifier. *Physical Review*, B 79(184301), 2009.

[3] Michael H. Devoret. Quantum fluctuations in electrical circuits. *Elsevier Science*, 1997.